Nanoscale

Accepted Manuscript

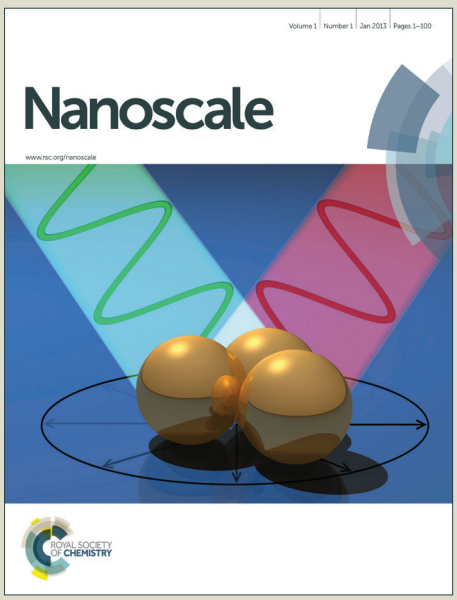

ROYAL SOCIETY OF CHEMISTRY

www.rsc.org/nanoscale

Cite this: DOI: 10.1039/c0xx00000x

www.rsc.org/xxxxxx

ARTICLE TYPE

Energy transfer processes in dye-doped nanostructures yield cooperative and versatile fluorescent probes

Damiano Genovese,*[a] Enrico Rampazzo,[a] Sara Bonacchi,[a,#] Marco Montalti,[a] Nelsi Zaccheroni,[a] and Luca Prodi[a]

Received (in XXX, XXX) Xth XXXXXXXXX 20XX, Accepted Xth XXXXXXXXX 20XX
DOI: 10.1039/b000000x

Fast and efficient energy transfer among dyes confined in nanocontainers is at the basis of outstanding functionalities in new-generation luminescent probes. This feature article provides an overview on recent research achievements on luminescent Pluronic-Silica NanoParticles (PluS NPs), a class of extremely monodisperse core-shell nanoparticles whose design can be easily tuned to match specific needs for diverse applications based on luminescence, and that have already been successfully tested in *in vivo* imaging. The outline of their outstanding properties, such as tuneable, bright and photoswitchable fluorescence and electrochemiluminescence, will be supported by critical discussion of our recent works in this field. Furthermore, novel data and simulations will be presented to (i) thoroughly examine common issues arising by the inclusion of multiple dyes in a small silica core, and (ii) show the emergence of a cooperative behaviour among embedded dyes. Such cooperative behaviour provides a handle for fine control on brightness, emission colour and self-quenching phenomena in PluS NPs, leading to significantly enhanced signal to noise ratio.

Introduction

Fluorescence-based methods are increasingly spreading in many fields of scientific and social relevance, spanning from the investigation of (bio)chemical mechanisms[1] and reactions [2] to material engineering,[3] to biological and medical applications, [4-6] including analytical assays, [7] diagnostics and so on. The reasons for their continuous development and applications can be found in their high time and space resolution, ease of revelation and use, relatively inexpensive equipment and in the versatility of fluorescence in adapting to extremely different experimental setups, always maintaining a high density of information. [8, 9]

The first direct consequence is an increasing call for new fluorescent probes, displaying innovative features: solubility adaptable to the individual application, higher brightness, tuneable emission wavelength, lifetime or anisotropy for multiplexing purposes, and switchable or responsive luminescent signals.

While molecular dyes need expensive and time consuming chemistry for modifications that accommodate different requirements, dye-doped nanostructures can permit a much more simple and versatile *modular* approach to meet different criteria by modifying their structure, their dye-content or their surface chemistry.[10, 11] In particular, PluS NPs, a type of core-shell nanoparticles prepared by co-condensation of tetraethylorthosilicate (TEOS) and alkoxysilane-derivatized dyes in micelles of the triblock copolymer Pluronic F127 in water,[12] represent an extremely valuable class of new-generation fluorescent probes. In fact, they show outstanding photophysical properties, they rely on an extremely easy and versatile one-pot preparation method, and their high water solubility and long-term stability make them suitable for bioanalysis and medical diagnostics *in vivo* and *in vitro*.[13-15]

In this article we will discuss our strategies to obtain novel and desired photophysical properties through steering a kinetic competition among valuable and detrimental deactivation paths, by means of energy transfer events. High local density of dyes in fact, stored in silica cores with diameter □ ~ 11 nm, triggers the activation of very fast energy transfer paths, as well as the formation of excimers and aggregates. Importantly, energy can be transferred also between identical dyes ("*homo*-FRET"), thus energy transfer processes can occur between donor and acceptor dyes that can be either different or equal to each other. The synergistic roles of *homo*- and hetero-FRET processes provide PluS NPs with relevant photophysical properties such as high brightness, tuneable fluorescence and electrochemiluminescence (ECL) colour, tuneable pseudo-Stokes shift and photoswitchable emission.

FRET-based nanostructured luminescent probes: enhanced photophysics as a result of collective behaviour

The ever increasing investigation methods based on fluorescence (microscopy,[16, 17] microfluidics,[18] bioanalytical assays[19] etc.) usually exploit traditional molecular fluorophores, with some exception in which semiconducting nanocrystals (QDs) and –quite rarely– other nanostructured fluorescent probes are used.

However, molecular fluorophores present many limitations, and the need to reach lower limit of detection (LoD) through enhancing the signal-to-noise ratio is a main motivation that leads chemists to design and use "more complex" systems based on luminescent nanostructured architectures.[20-22]

A major drawback of luminescent nanostructures, compared to molecular fluorophores, is that they often display complicate photophysical properties, including multiple emission bands, multiexponential lifetimes, and partial responses of such fluorescence parameters to external stimuli: why then seeking for collective behaviour, and thus for nanostructures acting as a whole? If dyes behave cooperatively, the change in the status of one dye can reverberate on many –up to all– other dyes present in the nanostructure, as depicted in Fig.1. This means that a single event (i.e. release of a proton, binding of an analyte, a thermally or chemically induced reaction, absorption of a photon and so on) is signalled by many dyes simultaneously, resulting in strong amplification effects (e.g. in sensing[23-25]), and to applicability in methods based on stochastic activation of fluorescent probes (superresolution microscopy,[26-28] enhanced-contrast imaging[29]).

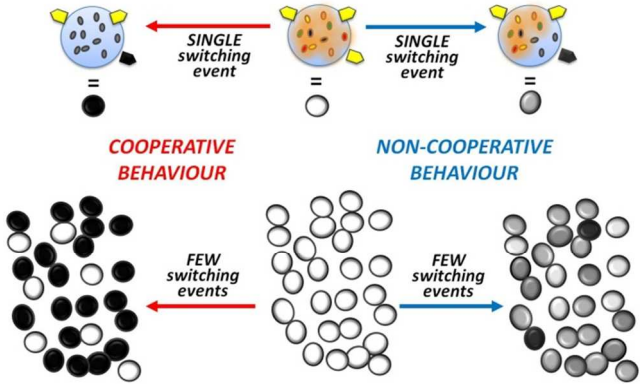

Fig. 1 Schematic depiction of cooperative and non-cooperative effects in dye-doped nanostructures. On top, the effect of a single event on a single nanostructure. The change of status of one responsive unit can affect only few dyes (right, non-cooperative behaviour) or the whole nanostructure (left, cooperative behaviour). Below, changing the status of several responsive units can result in either partial luminescence changes of each nanostructure (non cooperative behaviour, right) or strong changes of only some of them (cooperative behaviour, left).

Other common concerns on the use of nanostructures are linked to size limitations and toxicity issues. The size of luminescent nanostructures represents a major difficulty if labelled biomolecules are to preserve their diffusion properties or their biological activity. [30-32] Nonetheless, many targeted bio-recognition applications support the use of luminescent nanostructures,[11, 33] particularly when the fluorescently labelled biomolecules, membranes or tissues are neither expected to move, nor to perform any further functional activity. In such cases luminescent nanostructures, even if bulky and hindered, overcome molecular fluorophores in terms of enhanced signalling abilities and targeting specificity. [34] In the case of PluS NPs, focus of this feature article, their small size (hydrodynamic radius ~25nm) and their PEG shell guarantee effective extravasation as well as long circulation time and targeting capabilities of these probes also in vivo.[13, 15] Finally, nanostructures generally raise concerns on toxicity, but at the same time they offer significant keys of improvement due to a relatively easy surface chemistry that allows minimising undesired aggregation and accumulation in biological environments, which is the first requirement for cumulative and dangerous toxicity effects. PluS NPs have shown fast trafficking and excretion capabilities,[35] proving that its PEG surface is robust enough to resist various biological microenvironments and to guarantee fast expulsion rates.

The ultimate motivation for the intense research carried out on luminescent nanostructures can be found in the general race towards miniaturization, which characterizes most current academic and private research and investments. In fluorescence-based techniques, miniaturization means moving from bulk analyses down to single molecule experiments, passing through a plethora of low-volume –and low LoD– systems including immunoassays, arrays and microarrays, microfluidics and so on.[18, 36] The first evident requirement to allow this transition is an increase in brightness, together with reduction of interferences and noise: this motivates the contest towards ultrabright probes and towards amplification effects, and it is also at the basis of flourishing studies on (electro)chemiluminescent[37] and thermoluminescent[38] probes, which intrinsically eliminate the most significant source of interferences in fluorescence, i.e. the excitation source.

Nanostructures are often conceived as containers whose photophysical advantages arise from the ability of embedding many signalling units. This is true, but it is also only a first-level use: fluorescent units can be strongly interconnected within nanostructures to yield further advantages. In this feature article we focus on a special class of modular luminescent nanostructures based on a robust and versatile synthetic protocol which yields probes featuring ultrabright, tuneable fluorescence, as well as tuneable electrochemiluminescence, modular pseudo-Stokes Shift and photoswitchable emission. All these features have been achieved by interconnecting many kinds of dyes through efficient energy transfer pathways. *Homo*-FRET plays in PluS NPs a key role, since it boosts the overall efficiency of all other energy transfer processes, allowing such a variety of final photophysical properties. Excitation energy can indeed be distributed on several donor dyes by means of *homo*-FRET (within the relevant timescale) and eventually directed towards the fastest energy transfer pathways. The rates of energy transfer can be adjusted –to direct energy to the most useful pathways– by playing on relevant parameters such as interchromophoric distances and dyes spectral properties.

Förster Resonance Energy Transfer is indeed a long-time studied phenomenon that leads to deactivation of the donor excited state and excitation of the acceptor. Its probability is given by its kinetic competition with all other deactivation paths of the donor excited state, and it is thus determined by its characteristic rate k_{FRET}, which among other factors is proportional to the overlap integral J and to r^{-6}, as reported in equation (1)

$$k_{FRET} = \frac{Q_D \kappa^2}{\tau_D\, d(D-A)^6}\left(\frac{9000 ln10}{128\,\pi^5 N n^4}\right) J(\lambda) = \frac{1}{\tau_D}\left(\frac{R_0}{d(D-A)}\right)^6 \qquad (1)$$

d(D-A) being the donor-acceptor distance, and J being the overlap integral, i.e. the parameter that takes into account the matching between energies and probabilities of the two transitions at play, i.e. emission of the donor and absorption of the acceptor:

$$J(\lambda) = \int_0^{\infty} F_D(\lambda)\, \varepsilon_A(\lambda) \lambda^4 d\lambda \qquad (2)$$

where $F_D(\lambda)$ and $\varepsilon_A(\lambda)$ are the normalized fluorescence intensity and molar extinction coefficient spectra respectively, and λ the wavelength. The FRET phenomenon has been intensively studied and applied in many fields such as imaging,[39] as a "molecular ruler",[40] or as a tool to funnel energy in devices inspired to the antenna effect of natural leaves.[41, 42] The antenna effect, in particular, takes advantage of multiple FRET events, which can lead to transport of excitation energy: such transport, in the case of photosynthetic light harvesting complexes, is a highly organized process, which results in an extremely directional migration of the excitation energy from the periphery of the photosynthetic light harvesting complex to its reaction centre.

Nonetheless, in a non-organized ensemble of dyes such as in PluS NPs, FRET-based energy transport can still play a significant role and provide valuable properties and an efficient use of energy. A typical organic dye with a small fluorescence Stokes shift and high quantum yield, in fact, can easily possess a Förster Radius R_0 of about 5 nm for *homo*-FRET, [43] and consequently be able to transfer energy to other neighbouring molecules of the same type. This leads to a scenario where multiple energy transfer events can occur, leading to distribution of the excitation energy on many dyes within the excited state lifetime, as first described by Förster in 1946.[44]

In the following sections we will discuss how very fast FRET events occurring in PluS NPs determine and tune the photophysical properties of the whole nanostructures. Furthermore the reader can find hints on energy migration occurring within these nanoparticles. This phenomenon has a great relevance towards the important goal of obtaining homogenous photophysical properties which belong not to each individual dye inside the particle, but rather to the whole PluS nanoparticle, similarly to what happens for molecular dyes or QDs. As already mentioned, collective behaviour of encapsulated dyes is at the basis of the ability of these nanostructured luminescent probes to undergo strong amplification effects, which can pave the way to their use in high sensitivity methods, and where stochastic activation of fluorescent probes is required.

Structure of PluS NPs, a versatile fluorescent probe in nanomedicine

Condensation processes of silica precursors such as TEOS (tetraethylorthosilicate) or other organo-alkoxysilane represent a general and powerful approach to develop silica NPs in solution. Few different synthetic strategies give access to these systems, that stand out for the mild conditions and accessible synthetic procedures. The first milestone in this research field was placed by Kolbe[45] and then developed by Stöber in the late '60s,[46] exploiting TEOS hydrolysis and condensation promoted by ammonia in a mixture of ethanol and water.[47-49] Later, other strategies were developed,[50-55] focusing on the spatial control of the nucleation and silica core formation, either by means of a reverse microemulsion of surfactant and water in an hydrocarbon (water-in-oil methods),[56, 57] or through use of organo-trialkoxysilane derivatives and direct micelles suspensions of low molecular weight surfactants in water (ORMOSIL, ORganic-MOdified-SILica).[54, 58-60]

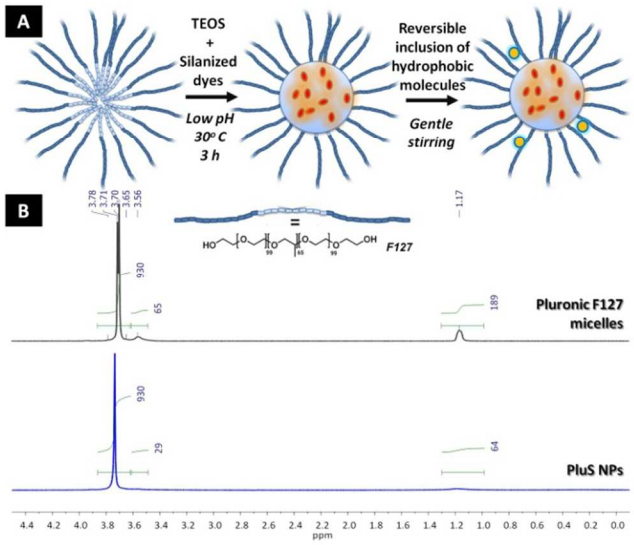

Fig. 2 A) Cartoon of the micelle-template synthesis. From left to right: Pluronic F127 micelles, PluS NPs, PluS NPs hosting hydrophobic molecules in the amphiphilic shell. B) ^{1}H-NMR spectra of Pluronic F127 (black) and of PluS NPs (blue). (400 MHz, D_2O, 25 °C), [61]reproduced by permission of The Royal Society of Chemistry.

Similarly to ORMOSIL NPs, PluS NPs are obtained with a direct micelles assisted method, using Pluronic F127 as surfactant. Its PEG-PPO-PEG amphiphilic structure (polyethyleneglycol-polypropylene oxide-polyethyleneglycol) and remarkable average molecular weight of 12.6 KDa, strongly contributes to the particular characteristics of these NPs.

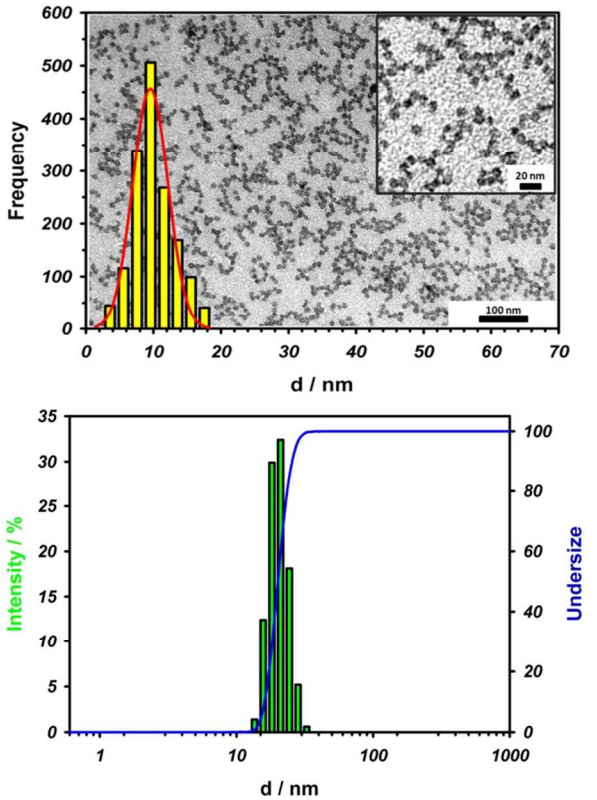

Fig. 3 Size distribution of PluS NPs according to TEM images (top) and DLS distribution in water (bottom). Adapted with permission from [35]. Copyright (2013) American Chemical Society.

Pluronic F127 forms quite large micellar aggregates in water (~ 22-24 nm) with a relatively polar inner core (PPO),[62] in which TEOS can be used as silica precursor instead of more lipophilic organo-alkoxysilanes, contributing to a more stable and dense silica network. The second advantage is that many kinds of alkoxysilane derivatized dyes, from polar to very lipophilic, can be used as doping molecules. More importantly this method distinguishes itself as a simple one-pot procedure yielding very monodisperse core-shell silica-PEG NPs. These NPs have a silica core of about 10 nm, and an overall hydrodynamic diameter of about 25 nm, as showed by TEM and Dynamic Light Scattering (DLS) measurements respectively.[63, 64] This structure was verified by other experimetal techniques, such as AFM measurements[64] that showed the co-localization of a soft shell and an harder silica core, and Thermo Gravimetric Analysis (TGA) which showed a fixed mass ratio between the organic and inorganic parts in samples subjected to ultrafiltration treatments (membrane cut-off 100 kDa) of different duration.[65]

The organization of the PEG-PPO portions of Pluronic F127 respect to the rigid silica core was also verified by ^{1}H-NMR measurements: only the most lipophilic central PPO portion of the triblock copolymer Pluronic F127 resulted strictly bounded to the central silica core of the particle, while the more hydrophilic PEG parts are outstretched toward the external water solution, in which they preserve most of their mobility. ^{1}H-NMR spectra of NPs suspensions indeed shows, compared to Pluronic F127 micelles in water (Fig.3), that the only decreased and broadened signals –typical of slowly diffusing units– are attributable to the PPO moiety (-OCH_2CHCH_3O-; -OCH_2CHCH_3O-; $\delta \cong 1.2$ and 3.6 ppm).[65]

Applications of PluS NPs as *in vivo* probes

The outstanding colloidal stability and morphological properties of PluS NPs make them ideal candidates for *in vivo* applications. Their PEG shell and tiny dimensions in particular provide them with high stability in presence of proteins, also compared to commercial hydrophilic QDs,[13] and guarantee a more dynamic behavior and long circulation times in *in vivo* imaging.[66]

Another added value of PluS NPs concerns functionalization aspects. With an equally simple one-pot procedure, but using co-aggregates of Pluronic F127 and of modified Pluronic F127 bearing suitable functional groups at the PEG ends, we proposed a high-performance imaging platform based on two-color emitting (red and NIR) PluS NPs, functionalized with colorectal cancer metastasis-specific peptides on the outer shell. The targeting specificity of such functional groups and the simultaneous detection of the signals, allowing background subtraction and signal amplification, resulted in high-sensitivity and high-specificity imaging.[15]

We have also investigated the effects of functionalized PluS NPs on cell endocytosis and cytotoxicity. Functionalized samples endowed with external amino- or carboxy-groups were safe and did not exhibit appreciable cytotoxicity in several normal or cancer cell types, growing either in suspension or in adherence. Flow cytometry studies demonstrated a more efficient cell uptake of amino-functionalized Plus NPs, with stable fluorescence signal associated to Plus NPs loaded cells populations both for *in vitro* and *in vivo* experiments settings.[14]

Finally, in a very recent work,[67] we showed how PluS NPs can be used to obtain efficient NIR emitting systems for regional lymph nodes mapping in mice. We developed two families of covalently Cy7 doped PluS NPs, bearing negative charge groups (-COOH) either at the periphery of PEG shell or directly bounded to the silica core, and hence characterized by different charge positioning schemes. The different location of charges in the core-shell nanostructure proved to have very deep influence in determining the PluS NPs kinetic behavior and their lymph node mapping capability. As a general indication, we quantitatively demonstrated that NPs bearing negative charges buried by a PEG shell were far more efficient that similar NPs having the same overall charge (ζ-Potential) exposed to the external environment. For the same system a non-toxic behavior both *in vitro* and *in vivo* was demonstrated, together with efficient excretion by hepatobiliary mechanism.

Simulating FRET in PluS NPs: the role of acceptor dyes and of Förster Radius

FRET efficiencies observed in PluS NPs are exceptionally high, as already shown in several published systems,[12, 68] and this is at the basis of innovative and collective photophysical properties. Such high experimental values are determined by the very close proximity among donor and acceptor dyes, arising from the high local concentration. At this stage it is unclear, though, whether a homogeneous distribution of dyes in the typical core of PluS NPs is consistent with these experimental observations. Furthermore, it still remains to be understood whether such high FRET efficiencies are consistent with one-step FRET from donor to acceptor, or if multiple intermediate steps between different donors –*homo*-FRET– should be taken into account.

It is worth noting that we expect PluS NPs to show quite a homogenous distribution of the embedded dyes in the core volume,[12] because they benefit of a completely different growth mechanism compared to the traditional Stöber method. In this latter synthetic strategy, a basic environment promotes nucleation processes[69], and different condensation rates of TEOS and alkoxysilane-dye derivatives determine an inhomogeneous distribution of the dyes in the particle;[70] on the contrary, PluS NPs grow under acidic conditions, which disfavour nucleation of colloidal silica[69] and make negligible the contribution of different condensation rates. This effect is strengthened by the high local concentrations reached in the confined nano-environment of Pluronic F127 micelles.

In the perspective of an increasingly incisive design of fluorescent probes on-demand, featuring specific photophysical properties, it is desirable to build up a strategy that consistently links a given choice of amounts and kinds of donor and acceptor doping dyes with the final fluorescence properties of the nanostructure. We have build up a simple simulation method, and tested it to predict FRET efficiency and thus spectral properties for given PluS NP "configurations", containing specific donor-acceptor couples, at given doping degrees. We have used it to quantitatively attest to what extent number of acceptor dyes and Förster Radius R_0 affect the overall (measurable) FRET efficiency.

Interchromophoric distances are calculated with a homemade

Matlab routine. A simple geometric model is used, in which PluS NPs cores are approximated to perfect spheres of 11 nm in diameter, and dyes are considered dimensionless points randomly dispersed in the inner volume. Calculations are run on a set of 1000 NPs (a number that ensures high reproducibility of the calculated parameters) in which dyes are Poisson distributed.[71] Orientation is only considered in average at this stage, through the orientational factor κ^2=0.476 theorized for a random arrangement of stationary molecules.[72]

After calculating all donor-acceptor distances we can extract relevant parameters for data analysis, in particular:

a) overall FRET efficiency for each donor dye:

$$\eta_{FRET}(D_i) = \kappa_{FRET}(D_i) \Big/ [\kappa_{FRET}(D_i) + \tau_D^{-1}] \quad (3)$$

where τ_D is the lifetime of the donor dye in absence of acceptors, and $\kappa_{FRET}(D_i)$ is the sum of the FRET rates of the ith donor dye towards each individual acceptor in the NP. Note that the distribution of $\eta_{FRET}(D_i)$ and its average value $\langle\eta_{FRET}\rangle$ can be readily compared with experimental data obtained from time-resolved and steady state fluorescence quenching measurements.

b) Average donor-acceptor distance. Such parameter can be not very meaningful if calculated as the simple mean, $\langle d\rangle$ since it does not change upon increasing the number of available acceptor dyes.

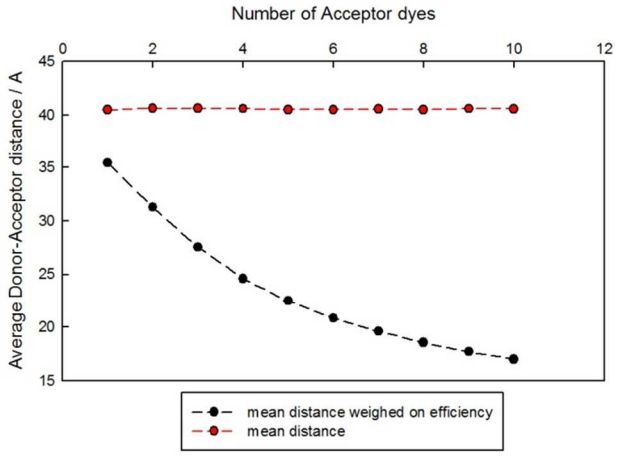

Fig. 4 Mean distance $\langle d\rangle$ (red dots) and mean weighted distance $\langle d\rangle_W$ calculated for a set of 1000 NPs containing 10 donor dyes in average and up to 10 acceptor dyes.

If such average donor-acceptor distance is instead weighted on FRET efficiency, we obtain $\langle d\rangle_W$, a relevant distance parameter that can be used to describe a multiple FRET system.

$$\langle d\rangle_W = R_0 \left[\sum_{a=0}^{Na} \left(\frac{R_0}{d_a}\right)^6\right]^{-1/6} \quad (6)$$

This weighted distance is obtained by combining equations 1 and 3; d_a is the distance between the donor and the a^{th} acceptor (over a total of *Na* acceptor dyes).

This new parameter correctly accounts for the presence of many acceptors for each donor, by giving different weights to the different dyes according to their distance. In fact, the acceptors act in parallel with a synergic effect on the donor quenching: the resulting increase in FRET efficiency is not paralleled by any change in the average donor-acceptor distance $\langle d\rangle$, but it is well matched by a decrease in the weighted average distance $\langle d\rangle_W$, as shown in Fig.4.

Interestingly, when FRET efficiency is calculated versus the number of acceptors and the Förster Radius, as mapped in Fig.5A, the importance of Poisson distribution of dyes is highlighted very clearly: very low FRET efficiency is in fact obtained with a very small number of acceptor dyes (up to 2 acceptors in average per particle). This is due to the significant fraction of particles that do not contain any acceptor dyes and in which the donor dyes are consequently unquenched. For example, 37 or 14 PluS NPs out of 100 have no acceptor dyes when particles contain respectively 1 or 2 dyes in average, as given by Poisson distribution:

$$P(N_i, \langle N\rangle) = \frac{\langle N\rangle^{N_i}\, e^{-\langle N\rangle}}{N_i!} \quad (7)$$

where $P(N_i,\langle N\rangle)$ is the probability to find a nanoparticle containing N_i dyes when $\langle N\rangle$ is the average number of dyes per particle.[71]

Furthermore, the efficiency map in Fig.5A shows that, when 4 to 6 acceptor dyes (for 4.0 nm < R_0 < 6.0 nm respectively) are embedded in average per particle, high FRET efficiency (> 90%) can be obtained. This is in quite good agreement, even if with little underestimation, with previously published data. [73]

The amphiphilic PEG shell is able to host hydrophobic molecules such as dyes or drugs. Such molecules are very close to the core and might then interact with core-embedded dyes. We simulated PluS NPs in which acceptor dyes are randomly dispersed in an increasingly thick shell, while the cores embed 10 donor dyes in average. The resulting average efficiencies $\langle\eta_{FRET}\rangle$, mapped in Fig.5B, are rather low (0.2 < $\langle\eta_{FRET}\rangle$ < 0.8), and are maximised only for large number of dispersed acceptor dyes in thin shell. These values are largely below experimental results,[68] suggesting that this simple model does not appropriately take into account an important part of the photophysical processes occurring in this peculiar class of fluorescent probes.

Next section will attempt to address these findings, showing that *homo*-FRET can be at the basis of extraordinary advances in fluorescent probe design.

Cite this: DOI: 10.1039/c0xx00000x

www.rsc.org/xxxxxx

ARTICLE TYPE

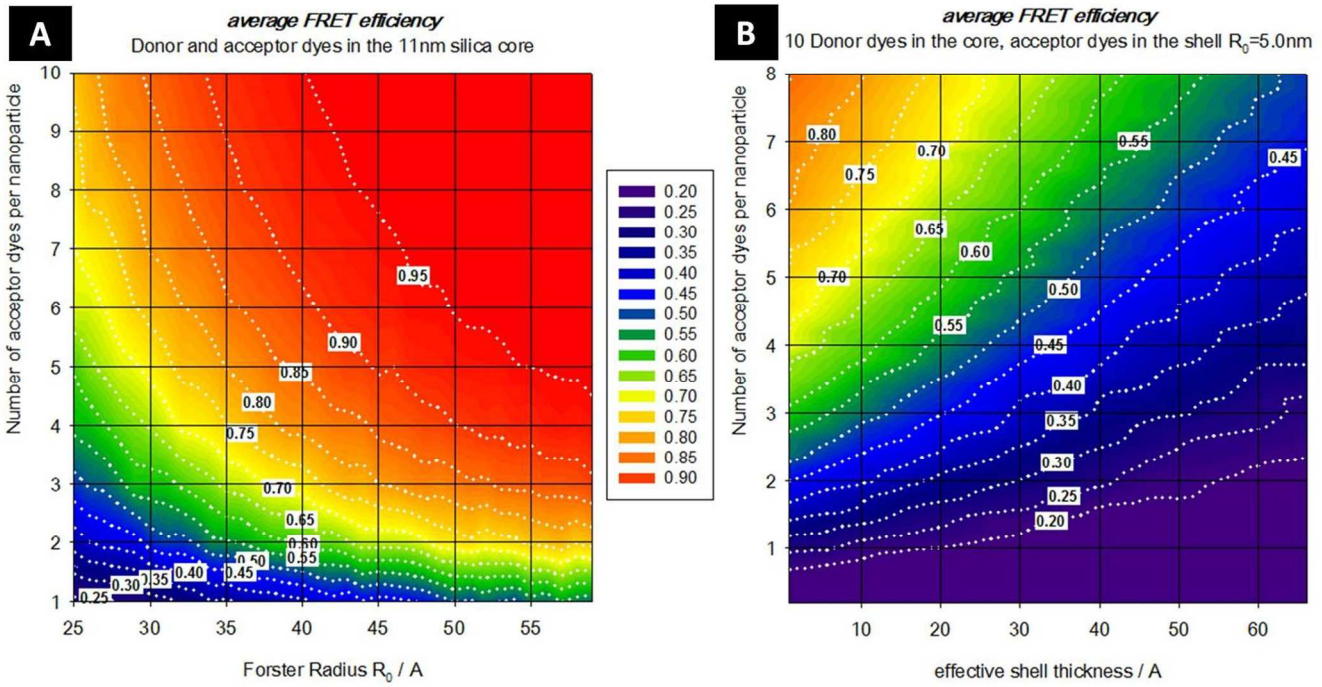

Fig. 5 Maps of average FRET efficiency $\langle \eta_{FRET} \rangle$ calculated with a Matlab routine based on a simple geometric model (description in the text). A) $\langle \eta_{FRET} \rangle$ is mapped versus Förster Radius R_0 and number of acceptor dyes, for a set of 1000 NPs containing 10 donor dyes in average embedded in a 5.5nm radius core, and an increasing number of acceptor dyes also randomly dispersed in the core. B) On the right, the same calculation has been run but with acceptor dyes randomly dispersed in an increasingly thick shell, and R_0 has been fixed to 5.0nm. $\langle \eta_{FRET} \rangle$ is mapped versus shell thickness and number of acceptor dyes. NB efficiencies are calculated for FRET from each individual donor dye to all available acceptor dyes, without considering energy transport by means of *homo*-FRET.

"*Homo*-FRET" distributes excitation energy: emergence of cooperative behaviour

When dyes with small Stokes Shift such as rhodamine, bodipy or cyanine are used to dope PluS NPs in quite high local concentration, the overall properties of these nanostructures cannot be correctly understood without considering excitation energy migration. Multiple FRET events in NPs result in distribution of the excitation energy in more than a single dye, up to all dyes embedded in the NP, within the lifetime of the excited state. Photophysical properties must then be evaluated by considering *collectively* all donor dyes in the NPs: it is not sufficient to weight the distances of all acceptors from each donor on FRET efficiency as in the parameter $\langle d \rangle^{Di}_{W}$ (as defined in eq. 6), but it is also necessary to take into account the simultaneous presence of the other donors. If excitation energy is on a slow pathway toward one of the acceptors (i.e. on a far donor), there exists the possibility to move to another donor dye, closer to an acceptor dye, which rapidly and efficiently funnels energy to it. In turn, the probability of the ith donor D_i to further exchange energy with other donors decreases with its ability to send it rapidly to the acceptors: a donor close to an acceptor makes excitation energy unavailable for further homoFRET steps, acting as the funnel that bridges homo FRET with FRET to acceptor dyes, with a net increase in the overall efficiency of this latter process.

The importance of such collective behaviour in dye-doped nanoparticles can be attested by considering the case of PluS NPs doped with rhodamine B dyes. We have shown in ref. [68] through analysis of time-correlated single photon counting (TCSPC) data and steady-state fluorescence measurements that the adsorption of a single cyanine dye per Plus NP causes a very strong quenching (~90%) of the fluorescence of all embedded rhodamines (~10 per NP). The cyanine dyes are reversibly hosted by the amphiphilic polymeric shell and are unlikely to penetrate the silica core. Most probably then these acceptor dyes, even if as close as possible to the silica core, can be even more than 10 nm away from some of the core-embedded donor dyes. As it has been shown with the aid of simulations, such high FRET efficiency would be out of reach simply considering each rhodamine dye as individually transferring energy to a cyanine ($\langle \eta_{FRET} \rangle$<80%, see Fig.5B and Fig.6). The gap to be filled among the experimental observations and a model that only accounts for FRET from individual donor dyes is shown in Fig.6.

Remarkably, we have found evidences of energy transport in PluS NPs from experimental measurements of emission anisotropy. In particular we have found that in PluS NPs doped

with ~ 4.5 dyes in average –covalently linked to the silica core–, the emission is depolarized by ~75% with respect to the excitation light (see following section). This means that the excitation energy adsorbed by each donor is distributed, during the excited state lifetime, on at least 4 dyes, i.e. on almost the totality of the embedded dyes.[44]

We believe it can be important here to report results on similar systems, i.e. dye-doped polymer films, where a different description, based on treating energy transport as a diffusive process, yielded typical experimental diffusion lengths in the range $5 < L_D < 30$ nm for dye concentrations in the range $10 <$ [dye] < 100 mM, which is also the range of local dye concentration in PluS NPs. [74-76] Such studies, though made on different matrices and in different conditions, confirm the trends observed in PluS NPs, where an efficient distribution of the excitation energy among many –up to all– donors in the silica core can finally explain experimental observations.

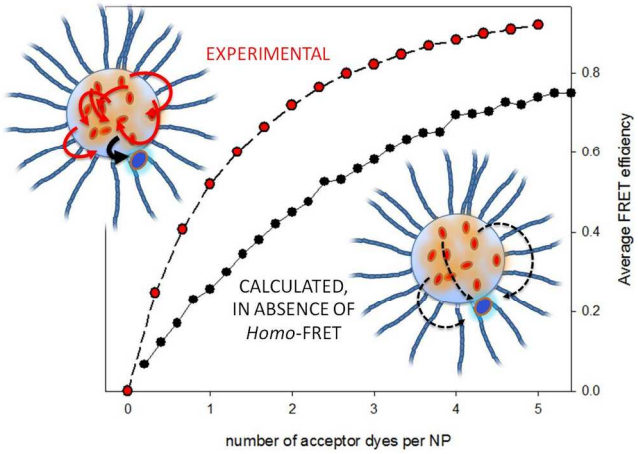

Fig. 6 Experimental FRET efficiency (red dots, obtained by steady state emission quenching measurements) versus simulated average FRET efficiency (black dots). No *homo*-FRET between donors is considered in simulations. Each point represents the average FRET efficiency for a set of 1000 NPs containing 10 donor dyes in average embedded in a 5.5nm radius core, and an increasing number of acceptor dyes hosted in a very thin shell (0.2nm). R_0=5.0 nm.

Remarkably, the collective behaviour of donor dyes in Plus NPs leads to several consequences that are very important for the application of such nanostructures, for example:

Fluorimetric titration can be used as an independent method to determine the concentration of PluS NPs solutions. Such new method can be extremely helpful in solving the common problem of determining NPs number concentration, which makes evaluations and comparisons with other probes rather difficult and vague.

Amplification of the response of fluorescent sensors can be achieved. In a previous study[24] a BODIPY-based sensor was hosted in the shell of PluS NPs doped with coumarin dyes, in stoichiometric ratio NP:dye=1:1. Complexation with Cu^+ ions increased the molar extinction coefficient of the sensor, as already previously observed. Consequently, addition of Cu^+ ions to coumarin-doped PluS NPs hosting sensors in the shell resulted in increasing the efficiency of energy transfer from a large number of donor coumarin dyes to a single acceptor sensor, thus affording a sensing response which was at the same time amplified and ratiometric.

This latter system proved that dye-doped PluS NPs can be employed as "excitation energy reservoirs", where the excitation energy adsorbed by many donor dyes embedded in the silica core can be used to amplify the fluorescence response of a complexation event occurring on a sensor hosted in the shell. Such strategy for signal amplification appears very effective also because noise is reduced with the increased separation between excitation and emission wavelengths, because it easily provides the possibility to apply ratiometric measurements, and, finally, because it can be potentially extended to a wide library of fluorescent chemosensors.

It is important to stress here that the main advances exhibited by PluSNPs, also in the field of fluorescent sensors, are based on the high level of cooperativeness among embedded dyes, which is due to the nanostructure: this allows a synergic action of all dyes –toward one mutual aim– rather than a mere cumulative effect of many dyes, each behaving individually, as is the case in most dye doped nanostructures.

Finally, the cooperative behaviour of dyes paves the way to other opportunities: we recently demonstrated[73] that a small amount of acceptor dyes are indeed able to catch energy from a large amount of donor dyes before poorly emitting states are populated. In the next paragraphs we will show that such a kinetic competition offers a strategy to circumvent the detrimental effects of self-quenching, raising the threshold for maximum doping degree with maintaining a continuous increase in brightness.

Effects of increasing dye doping: issues and solutions

Among the main reasons that motivate the effort to move from molecular fluorescent systems to luminescent nanostructures there is the possibility to embed a large amount of dyes, and to scale properties such as the absorption cross section and the brightness with the number of included dyes. The intensity of the fluorescence signal can thus be in principle enhanced by the presence of multiple dyes in one signalling unit (the nanostructure), yielding highly fluorescent markers for many applications.

Typically, if self-quenching processes do not occur, inclusion of hundreds to thousands of dyes –with proportional increase in brightness– can be achieved with particles as large as 30-100nm.[77] Cell inclusion, membrane permeability, and labelling of biomolecules and of nano-objects are common applications that have stringent size requirement, often setting an upper threshold of 10-30nm in diameter for fluorescent nanostructures to prove useful.

In this size range, the number of dyes that can be embedded – while maintaining a gain in the fluorescent signal– is much smaller, typically tens to hundreds of dyes. [12, 78, 79] We have performed systematic studies on photophysics of dyes in PluS NPs, which have a core of only 10nm in diameter. In particular, we investigated the effects of increasing the dye doping degree on the photophysics of the NPs.

Increasing local dye concentration: anisotropy drops, self-quenching increases and broadens fluorescence decay distribution

Rhodamine B is an exemplary xanthene dye, a class of dyes commonly used in most fluorescence based analysis and imaging applications.[80] It is well known to undergo formation of dimers and aggregates with poor photophysical features (low quantum yield, low brightness) at high local concentration.[81] We prepared PlusNPs covalently doped with increasing percentage of rhodamine B with respect to TEOS (0.1%, 0.25%, 0.5%, 0.75% and 1% moles of dyes vs moles of TEOS, correspondingly to approximately 4.5, 10, 20, 30 and 40 dyes per PluS NP respectively), by adapting a previously reported procedures with the desired amount of the silane-dye derivative.[68] We did not observe any leaking or incomplete dye inclusion in this concentration range, and in fact the absorption spectra revealed very good linear correspondence between nominal doping degree and per-particle molar extinction coefficient, except for minimal spectral distortions in the two more concentrated samples evidencing some formation of dimers and aggregates at the ground state (data not shown).

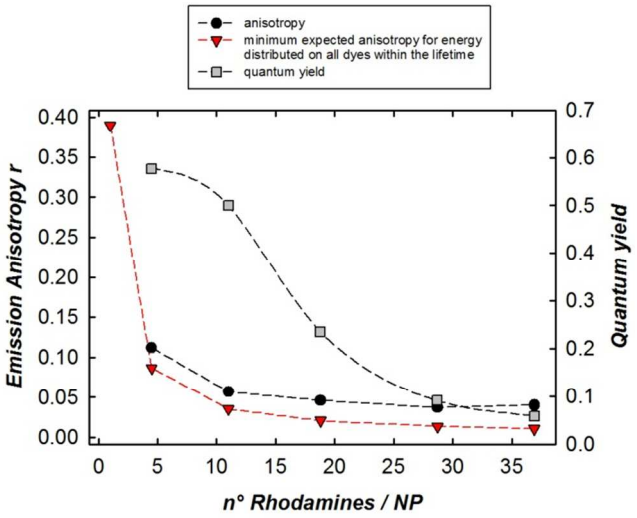

Fig. 7 Gray squares: quantum yields of PluS NPs at increasing doping degree (right ordinate axis); Black circles and red triangles: respectively experimental fluorescence anisotropy, and calculated minimum anisotropy for excitation energy distributed over all donor dyes present in the NPs (left ordinate axis).

Luminescence spectroscopy techniques[‡] reveal the higher sensitivity of excited states to the presence of nearby dye molecules, compared to ground states. In fact, the average quantum yield of rhodamine dyes in PluS NPs changes much more steeply with loading than the molar extinction coefficient, exhibiting a significant drop at a concentration of 20 dyes per particle (Fig. 7). Multiplication of the average quantum yield and the molar extinction coefficient of each PluS NP sample yields the expected brightness of these nanostructures (defined as $B=\Phi*\varepsilon$), which can be easily compared with experimental data obtained by fluorescence spectra of equimolar solution of **R+NPs** samples measured with constant instrumental settings (Fig. 10). The most sensitive property to the increase in doping percentage is, however, fluorescence anisotropy. Anisotropy was reduced by ~75% at the lowest doping degree (corresponding to ca. 4.5 dyes per NP) compared to the fundamental value of 0.39 (measured in a 95:5 glycerol:water mixture (v:v), containing ca. 0.5 mM NaOH[82, 83]) expected for rhodamine B in a rigid matrix with low rotational diffusion coefficient, as in PluS NPs. Moreover, this parameter decreases almost to its minimum value already at the doping degree of 10 dyes per particle. The number of energy transfer steps is indeed expected to increase with the square of the local dye density.[44] This proves that fast *homo*-FRET is at play at very low doping degrees –even lower than 5 dyes per particle–, while self-quenching, ascribable to the massive formation of poorly emitting states, only occurs at higher local dye concentration (>10 dyes per PluS NP). It is worth noting that also this experimental information strongly supports the existence of fast pathways for energy migration within PluS NPs, whose importance has been discussed and underlined in previous paragraphs.

As a consequence of the formation of poorly emitting aggregates, intrinsically uncontrolled and unequal in the individual NPs, the most highly doped samples show inhomogeneous and polydisperse photophysical behaviour. Fluorescence decays are in fact increasingly multiexponential as a result of the distribution of poorly emitting excited states (Fig.8).

In summary, rhodamine B dyes covalently linked to the silica matrix of PluS NPs exhibit intense communication by means of energy transfer which leads to depolarization of fluorescence respect to the excitation. The number of energy transfer steps increases with increasing the number of embedded dyes, resulting in complete depolarization at the low doping degree of 0.25%. If the doping degree is further increased, the formation of poorly emitting or completely quenched aggregates is observed. Such aggregates, acting as energy traps, are populated by other dyes by means of energy transfer events, with consequent depletion of quantum yield and brightness of PluS NPs, which is detrimental for their application potential as fluorescent labels.

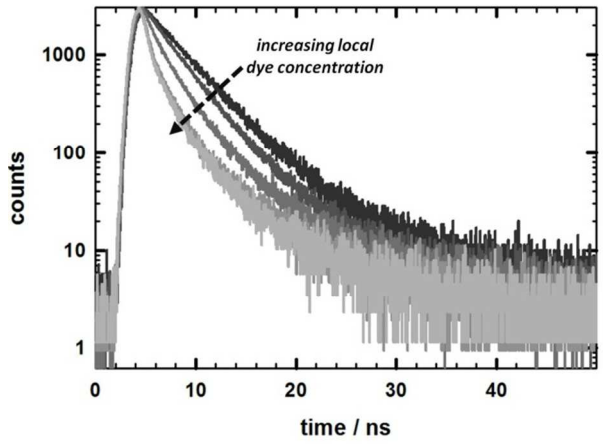

Fig. 8 Fluorescence decays of Plus NPs doped with up to ~40 rhodamine B dyes per particle. The lifetime becomes increasingly multiexponential, and the average lifetime decreases, with increasing number of dyes per particle.

Cooperative behaviour provides a strategy to overcome self-quenching

Until now the only solution to self-quenching has been to limit the doping percentage below a certain threshold. The actual threshold value was found to depend on several parameters, such as:

1) *preparation method*: homogenous solution based methods, such as Stöber method, often generate a concentration gradient of

the encapsulated dyes along the particle radius, resulting in distributed photophysical properties [84]

2) *intrinsic dye geometry and steric hindrance*: formation of dimers and aggregates largely depends on the geometry of the molecule, and it is favoured by large and flat conjugated planes which trigger π–π stacking interactions; nonetheless, such interactions can be efficiently avoided by increasing the steric hindrance of the dye molecules[85-87]

3) *intrinsic electronic properties of the dyes*, and specifically the Stokes Shift. Kell et al[88] showed that dyes featuring large Stokes Shifts could be generally loaded at higher threshold values than dyes with small Stokes Shift.

To contrast these poorly emitting states acting as traps for the excitation energy, we have exploited the confined space of Plus NPs to boost FRET pathways that divert excitation energy towards bright acceptor dyes, acting as "good" traps.

We prepared fluorescent PluS NPs doped with a coumarin derivative at different molar ratios with respect to TEOS, and we obtained PluS NPs doped with approximately 5 to 40 dyes per NP. Such dyes were quantitatively embedded in the silica cores, but the resulting fluorescence properties exhibited a strong dependence on the number of embedded coumarin: a gradual red shift of the emission maximum and the rise of a new excimeric band at around 550 nm were observed at high doping percentages, concurrently with a drop in the fluorescence quantum yield.

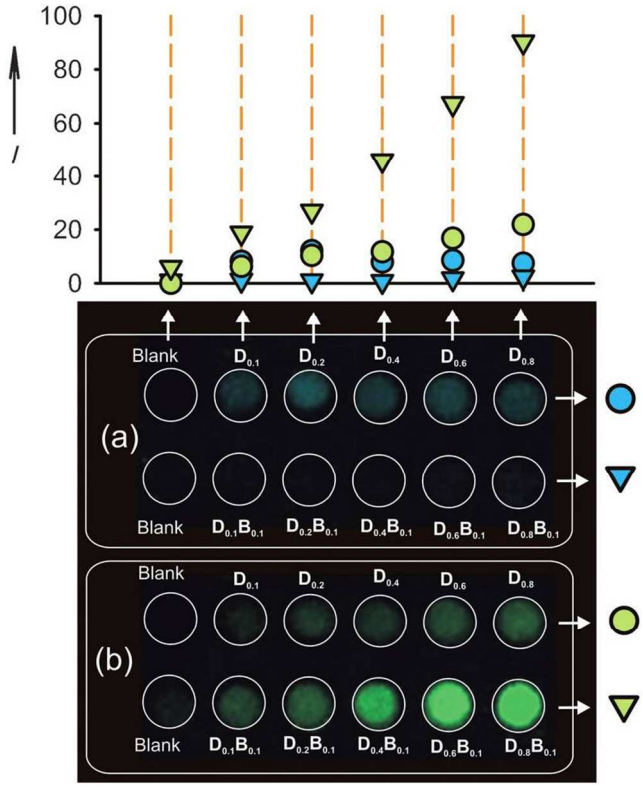

Fig. 9 Fluorescence imaging test to evaluate brightness. In figures a and b millimetre sized wells containing isoconcentrated water suspensions of PluS NPs increasingly doped with coumarin dyes (upper rows) or also embedding a small amount of bodipy dyes (lower rows). The signal is recorded with a CCD camera upon excitation at (390±9) nm, by using either a blue emission filter (460±30nm, a) or a green emission filter (530±22nm, b). On top, total intensities are integrated and plotted

As mentioned above, our strategy to avoid self-quenching is based on energy transfer: an energy acceptor, whose quantum yield and spectral properties are not affected by neighbouring coumarin dyes, is embedded in the NPs, in order to catch the excitation energy while it is exchanged among the donor coumarin dyes, in competition with the formation and deactivation of the poorly emitting states. It was found that very few bodipy dyes (~ 5), chosen as the acceptors, were able to collect almost the total energy absorbed by the numerous coumarin dyes (up to ~ 40): such highly efficient energy transfer, overcoming the formation of poorly emitting states, yielded increasingly bright PluS NPs, characterized by almost no energy loss. Furthermore, improved spectral emission properties were obtained with the bodipy moieties, because the rather broad fluorescence band typical of coumarins aggregates was turned into narrow bodipy emission and shifted at higher wavelengths. This phenomenon can be seen as a significant increase in a "pseudo-Stokes Shift", which can be defined as the energy difference among the *main* absorption peak (the one of the numerous donor dyes) and the main emission peak (the emission of the acceptor).

The concomitant increases in brightness and pseudo-Stokes Shift offered by these materials lead to a straightforward and significant breakthrough in the signal-to-noise ratio, paving the way to a general design strategy for new-generation fluorescent probes.

It is now of interest to establish whether the strategy just discussed is general or limited to the reported case, and whether it is a pure photophysics-based process, or rather determined by chemical interactions among the dyes. Is it possible to exclude a role of the acceptor dyes, during the synthesis of the nanostructure, in avoiding the formation of aggregates of the donor dyes and poorly emitting species?

We have designed a new experiment to answer such questions, based on previously reported observations that proved that (a) a cyanine dye can be efficiently included in the hosting PEG shell of PluSNPs, and that (b) it is extraordinarily efficient in accepting energy from all rhodamine dyes embedded in the core of PlusNPs.[68]

In the present experiment we added equal amounts of the same cyanine dye to the whole set of rhodamine doped PluS NPs previously discussed, doped with an increasing number of rhodamine dyes (range ~4-40 dyes per NP). The chosen amount of acceptor dye was 7.5 cyanines per PluS NP, which ensures an almost quantitative quenching of all rhodamines in all samples (Fig.10B). Note that, as extensively discussed in [68], one cyanine can be efficiently sensitized by all donors embedded in a PluS NP doped with 10 rhodamine dyes; we chose to add a slightly larger amount for two reasons: 1) to ensure that, following Poisson statistics, *at least* one cyanine dye is present in each PluS NP, and also 2) to increase the number of available paths for FRET and thus increase the overall FRET rate (see Fig.5B), which is particularly important for the most highly doped NPs in which the kinetic competition for the excitation energy is harshest.

Noteworthy, the acceptors are in this case added in the external PEG shell, after the preparation of dye-doped PluS NPs. This

procedure rules out the possibility of chemical interactions among donor and acceptor dyes being at the base of avoided self-quenching, proving that the excitation energy is recovered by a purely photophysical process. Furthermore, rhodamine dyes do not show any new emission band, even at the highest local concentration in the most heavily doped NPs. In turn, the fluorescence decays are significantly shortened, proving the formation of quenched states which have shorter decay times and quench the most fluorescent rhodamine dyes.

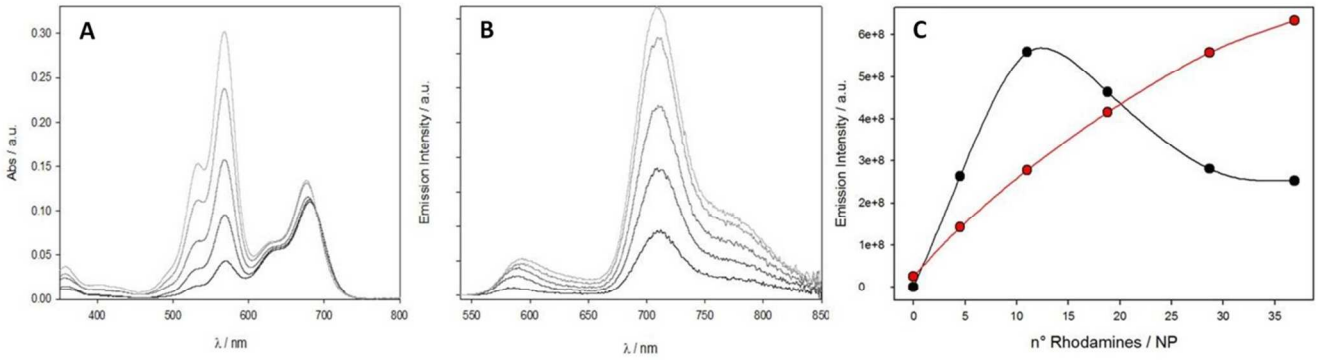

Fig. 10 A- Absorption spectra of PluS NPs doped with up to ~40 rhodamine dyes per particle, after addition of ~7.5 cyanine dyes per particle. B- Emission spectra of the same samples as in A, λ_{exc}=535nm. C- Brightness as the integrated emission spectra of PluS NPs doped with up to ~40 rhodamine dyes per particle (black dots) and after addition of ~7.5 cyanine dyes per particle (red dots), λ_{exc}=535nm.

Fig.10C shows the brightness trend, upon prevalent excitation of rhodamine dyes (λ_{exc}=535nm), as a function of rhodamine doping degree when cyanine is not present (black dots) and after its addition (red dots). In the first case we recognize the typical trend in which raising the number of dyes after a certain threshold results to be strongly detrimental for the brightness of the system. On the contrary, when cyanine acceptors are hosted in the shell of PluS NPs, we observe an almost complete quenching of rhodamine fluorescence and, more importantly, also an almost linear increase of the emission intensity as a function of donor dyes concentration. Note that the difference in slope at less than 10 dyes per particle is due to the difference in quantum yield between the two emitting dyes (cyanine has roughly 66% the quantum yield of rhodamine[68]). This demonstrates that cyanine dyes are effective in gathering all the energy absorbed by rhodamine dyes, thus also the fraction that would otherwise be "lost" in self-quenching processes.

This experiment thus supports the general effectiveness of our strategy to circumvent self-quenching, based on setting up a kinetic competition in which FRET to an unquenched acceptor overcomes formation and deactivation of poorly emitting aggregates.

FRET in PluS NPs provides versatile application

Enhancing resolution and contrast: photoswitchable FRET

One of the most intriguing development areas in the field of fluorescent markers is related to the possibility of switching fluorescence signals on and off, which among other applications constitutes the basis for most super-resolution fluorescence imaging techniques. Furthermore, the possibility of modulating fluorescence intensity allows an efficient subtraction of undesired interfering signals –which are normally constant in time–, as clearly and more extensively explained in [29]. Super-resolution imaging techniques share a common idea: using information from several diffraction-limited images to create one super-resolved image. The diffraction limit can be in fact overtaken if an ensemble of emitters, though not moving within a certain number of frames, changes its global appearance by partially turning on and off intermittently, and thus offering the possibility to reveal sub-diffraction features with suitable algorithms.[26-28, 89]

On the one hand, many efforts are at present dedicated to the development of new algorithms and instrumental setups, but on the other hand all these efforts rely on the fundamental need for new advanced switchable fluorescent probes, with stringent requirements on their brightness, on the signal difference between the on and off states, and on the possibility of tuning frequency and residence times of the fluorescent probes in such on and off states. Such photophysical properties in fact necessarily determine –and limit– the performances of super-resolution techniques.

Among the attempts that have been made to overcome the use of photoswitchable molecular dyes, which notoriously display drawbacks such as limited brightness, environment-dependent photophysical properties, lengthy and expensive synthetic procedures to adjust solubility -which is often poor in water-, we want to mention some findings concerning the use of QDs, polymer dots, dendrimers and PluS NPs.

QDs exhibit unique photophysical properties such as broad excitation, narrow emission, high photostability, and high brightness. Nonetheless the attempts to modulate their luminescence has given until now not fully satisfactory results, with photochromic FRET leading to less than 35-40% of QDs luminescence quenching, and fatigue resistance typically limited to 10-20 photoconversion cycles, probably due to irreversible electron transfer events. [90-93]

Polymer dots recently have emerged as a new class of ultrabright fluorescent probes with promising applications in biological detection and imaging. Several attempts have been performed to couple fluorescent conjugate polymers to photochromic dyes, which in most cases were only partially successful, since the photoswitchable fluorescence was affected by irreversible photobleaching of the polymer luminescence,[94] or by very low quantum yield of polymer dots (Φ~0.01), or by leaching of the embedded photochromic dyes from the polymeric

assemblies.[95, 96] An interesting solutions was found by Chiu et al.,[97] who developed photoswitchable polymer dots by conjugating photochromic spiropyran molecules and PFBT. They observed quenching of the polymer luminescence to only 14% of the initial intensity, but they achieved such result only using a quite high number of photochromic dyes per fluorescent unit of the polymer chains (approximately 8-10 photochromic dyes per fluorescent unit), and such efficient on-off cycles could only be repeated for around 10 cycles.

More complex approaches based on crosslinking dendrimers through a functionalized photochromic dye to obtain dendiritic nanoclusters hosting fluorescent dyes have not led to substantial advances in the performances of photoswitchable fluorescent probes, since the most efficient device displayed only 47% reduction in the initial fluorescence intensity.[98]

As for dye-doped nanoparticles, consisting of an inert matrix (silica or polymer -polystyrene, polymethylmethacrylate-) in which fluorescent and photochromic dyes are separately dispersed, only partial quenching has been observed, leading in some cases to multipeak luminescence, of interest for barcoding applications in which the barcoded emission signal is modulated through light irradiation. Very strong quenching (~90%) was obtained only by doping the particles with a large excess of the photochromic dyes compared to the fluorescent ones (in the range of hundreds photochromic per fluorescent dye).[99, 100]

The innovative architecture of PluS NPs has proven useful to realize versatile nanometric photoswitchable fluorescent probes of simple preparation. The amphiphilic outer shell allows reversible hosting of hydrophobic molecules in water,[68, 101] a property which was exploited to reversibly insert a photochromic dithienylethene derivative in rhodamine-doped PluS NPs. The ability of such photochromic dye to accept energy from the dyes buried in the silica core was proven to depend on its (open or closed) form, and thus on irradiation with UV or visible light. The emission spectrum of the rhodamine-doped PluS NPs, indeed, did not change in shape upon UV irradiation, but its intensity was drastically reduced to roughly 5% of the initial intensity, proving that a very efficient –and unprecedented in the field– energy transfer processes had been triggered on. The inverse process took place by irradiating with visible light, fully recovering the initial fluorescence intensity. This process was achieved with approximately a 1:1 ratio of fluorescent and photochromic dyes, it could be repeated tens of times with only minor changes, and it was also successfully tested in a wide-field fluorescence microscope setup. Notably, this approach is extremely easy and versatile, since it can be applied to any kind of dye-doped PluS NPs with –in principle– most available photochromic dyes.

In conclusion, PluS NPs offer an extremely interesting alternative to photoswitchable molecular dyes, also compared to similar attempts that have been performed with other luminescent nanostructures. Nonetheless, major improvements in this context are still to be addressed, and must be sought, apart from a necessary enhancement of the photostability of these probes, in (i) increasing the signal difference between on and off states and (ii) using down to a single photochromic dye. Concerning this latter point, molecular photoswitches have indeed the unique property that a single photoswitching event corresponds to the whole achievable brightness modulation of the fluorescent probe itself. This is extremely useful in all superresolution methods based on stochastic switching of the fluorescent probes. On the contrary, up to now nanoparticles need several switching event to reach the maximum achievable quenching (or brightness recovery), with the consequence that stochastic photo-activation of a pattern of fluorescent nanoparticles results in a partial fluorescence recovery or quenching distributed on all probes, rather than an abrupt fluorescence signal change of a fraction of the fluorescent probes. This is in our opinion the most important gap to be filled to start a real application of fluorescent probes based on nanoparticles in the field of superresolution microscopy, which can only be filled with a strong inter-dye communication, leading to large amplification effects.

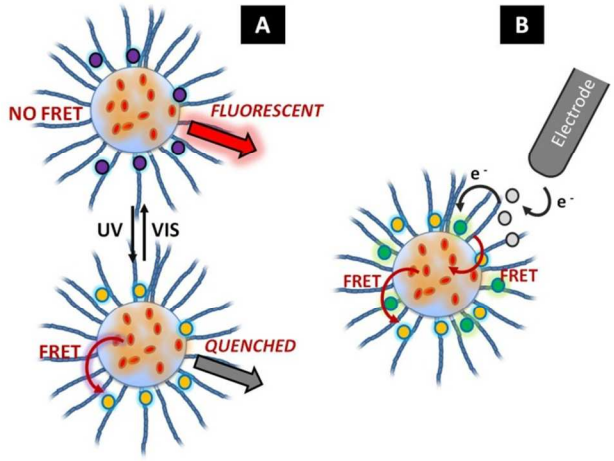

Fig. 11 A- Cartoon of photoswitchable PluS NPs. B- Cartoon of ECL-active PluS NPs whose emission colour can be tuned via FRET

We believe that PluS NPs, among few other reported examples of nanomaterials[102], have the potential to do it, since in several cases a strongly collective behaviour has been observed as already discussed in this article.

Making ECL versatile: electrochemically triggered FRET

In electrochemiluminescence (ECL), the emitting excited state is produced via a series of electrochemical reactions, so that luminescence is triggered by the electrode without the need of a light source. The possibility of avoiding excitation sources can lead to remarkably low noise, signal specificity, and different design of the luminescent device. Such peculiar properties make ECL particularly intriguing for commercial assays in very important areas, such as clinical diagnostics, food and water testing, and environmental monitoring.

For most clinical and environmental applications water solubility and the presence of suitable binding sites for bioconjugation are nowadays stringent requirements that need to be met by the luminophore, beside an intense and stable ECL signal. These conditions restrict very much the number of possible candidates and ruthenium polypyridine complexes (in particular, $Ru(bpy)_3^{2+}$) are nowadays practically the only luminophores so far employed in the commercial applications of ECL.

PluS NPs are the first nanostructures in which (i) ECL from non-water soluble ECL-active dyes has been observed,[61, 103] and

which allowed (ii) colour tuning of the electrogenerated emission through FRET between an ECL-active donor dye and one or two fluorescent dyes in cascade, excluding some examples of ligand modification as in [104] . Valenti et al. reported in fact the successful realization of the first example of a nanoparticle-based ECL-FRET system made of PluS NPs embedding up to three dyes in cascade, among which the highest in energy was efficiently excited via an electrochemical reaction (a common and robust ECL-active dye, diphenylantracene), which in turn was quenched by two dyes in cascade, resulting in an electrogenerated signal tuneable with the inclusion of acceptor dyes at lower energy. The reported electrochemically triggered FRET occurred, with high efficiency, among dyes hosted in the external shell, from dyes hosted in the shell to dyes hosted in the core and vice versa.

Such strategy, based on electrochemically induced energy transfer, afforded tuneable emission colour, without the need of synthesizing new ECL dyes. These findings showed that the use of PluS NPs can enlarge the library of dyes (and colours) suitable for ECL applications, making multiplex analysis easier to attain in the near future, increasing the already high potential of the ECL technique.

Conclusions

In conclusion, we presented a class of nanostructured fluorescent probes –PluS NPs– whose photophysical properties can be varied to respond to very different requirements and to be successfully employed in many methods based on luminescence. Such versatility is based on efficient energy transfer processes that can be tuned to steer the excitation energy towards the most valuable pathways.

A simple geometric model, supported by experimental observations, attested that *homo*-FRET plays a prominent role in distributing excitation energy among several donor dyes, and thus making it available for the final processes of interest. Dyes behave then cooperatively, so that the change in the status of one dye can reverberate on many –up to all– other dyes present in the nanostructure, leading to strong amplification effects. Probes featuring tuneable, bright and/or photoswitchable fluorescence or electrochemiluminescence are obtained.

Finally, due to their outstanding colloidal stability and morphological properties, PluS NPs have proved to be ideal candidates for *in vivo* applications.

Notes and references

[a] *Dipartimento di Chimica "Giacomo Ciamician", via Selmi 2, Bologna, 40126, Bologna, Italy. E-mail:damiano.genovese2@unibo.it*

[#] *Current address: Nanochemistry Laboratory, ISIS & icFRC, Université de Strasbourg & CNRS, 8 allée Gaspard Monge, 67000 Strasbourg, France.*

‡ Details on photophysical measurements can be found in [68].

1. M. Przybylo, T. Borowik and M. Langner, *J Fluoresc*, 2010, **20**, 1139-1157.
2. T. Tachikawa and T. Majima, *Chem Soc Rev*, 2010, **39**, 4802-4819.
3. M. Schaferling, *Angew Chem Int Ed Engl*, 2012, **51**, 3532-3554.
4. S. A. Claridge, J. J. Schwartz and P. S. Weiss, *Acs Nano*, 2011, **5**, 693-729.
5. T. L. Doane and C. Burda, *Chem Soc Rev*, 2012, **41**, 2885-2911.
6. K. Eggenberger, N. Frey, B. Zienicke, J. Siebenbrock, T. Schunck, R. Fischer, S. Bräse, E. Birtalan, T. Nann and P. Nick, *Advanced Engineering Materials*, 2010, **12**, B406-B412.
7. D. M. Jameson and J. A. Ross, *Chem Rev*, 2010, **110**, 2685-2708.
8. U. Resch-Genger, K. Hoffmann, W. Nietfeld, A. Engel, J. Neukammer, R. Nitschke, B. Ebert and R. Macdonald, *J Fluoresc*, 2005, **15**, 337-362.
9. M. I. Stich, L. H. Fischer and O. S. Wolfbeis, *Chem Soc Rev*, 2010, **39**, 3102-3114.
10. H. Kobayashi, M. R. Longmire, M. Ogawa and P. L. Choyke, *Chem Soc Rev*, 2011, **40**, 4626-4648.
11. J. Rao, *Acs Nano*, 2008, **2**, 1984-1986.
12. S. Bonacchi, D. Genovese, R. Juris, M. Montalti, L. Prodi, E. Rampazzo and N. Zaccheroni, *Angew. Chem.*, 2011, **50**, 4056-4066.
13. E. Rampazzo, F. Boschi, S. Bonacchi, R. Juris, M. Montalti, N. Zaccheroni, L. Prodi, L. Calderan, B. Rossi, S. Becchi and A. Sbarbati, *Nanoscale*, 2012, **4**, 824-830.
14. E. Rampazzo, R. Voltan, L. Petrizza, N. Zaccheroni, L. Prodi, F. Casciano, G. Zauli and P. Secchiero, *Nanoscale*, 2013, **5**, 7897-7905.
15. M. Soster, R. Juris, S. Bonacchi, D. Genovese, M. Montalti, E. Rampazzo, N. Zaccheroni, P. Garagnani, F. Bussolino, L. Prodi and S. Marchio, *Int J Nanomedicine*, 2012, **7**, 4797-4807.
16. H. R. Petty, *Microsc Res Tech*, 2007, **70**, 687-709.
17. J. W. Lichtman and J. A. Conchello, *Nat Methods*, 2005, **2**, 910-919.
18. H. H. Gorris and D. R. Walt, *Angew Chem Int Ed Engl*, 2010, **49**, 3880-3895.
19. C. Hempen and U. Karst, *Anal Bioanal Chem*, 2006, **384**, 572-583.
20. K. Wang, X. He, X. Yang and H. Shi, *Accounts of Chemical Research*, 2013, **46**, 1367-1376.
21. C. Wu and D. T. Chiu, *Angew Chem Int Ed Engl*, 2013, **52**, 3086-3109.
22. C. McDonagh, O. Stranik, R. Nooney and B. D. MacCraith, *Nanomedicine*, 2009, **4**, 645-656.
23. S. Bonacchi, E. Rampazzo, M. Montalti, L. Prodi, N. Zaccheroni, F. Mancin and P. Teolato, *Langmuir*, 2008, **24**, 8387-8392.
24. E. Rampazzo, S. Bonacchi, D. Genovese, R. Juris, M. Sgarzi, M. Montalti, L. Prodi, N. Zaccheroni, G. Tomaselli, S. Gentile, C. Satriano and E. Rizzarelli, *Chemistry*, 2011, **17**, 13429-13432.
25. L. Basabe-Desmonts, D. N. Reinhoudt and M. Crego-Calama, *Chem Soc Rev*, 2007, **36**, 993-1017.
26. E. Betzig, G. H. Patterson, R. Sougrat, O. W. Lindwasser, S. Olenych, J. S. Bonifacino, M. W. Davidson, J. Lippincott-Schwartz and H. F. Hess, *Science*, 2006, **313**, 1642-1645.
27. T. Dertinger, R. Colyer, G. Iyer, S. Weiss and J. Enderlein, *Proceedings of the National Academy of Sciences of the United States of America*, 2009, **106**, 22287-22292.
28. M. J. Rust, M. Bates and X. Zhuang, *Nature Methods*, 2006, **3**, 793-795.
29. Z. Tian and A. D. Q. Li, *Accounts of Chemical Research*, 2013, **46**, 269-279.
30. M. Mahmoudi, I. Lynch, M. R. Ejtehadi, M. P. Monopoli, F. B. Bombelli and S. Laurent, *Chem Rev*, 2011, **111**, 5610-5637.

31. P. R. Leroueil, S. Hong, A. Mecke, J. R. Baker, Jr., B. G. Orr and M. M. B. Holl, *Accounts of Chemical Research*, 2007, **40**, 335-342.
32. J. B. Delehanty, H. Mattoussi and I. L. Medintz, *Anal Bioanal Chem*, 2009, **393**, 1091-1105.
33. J. E. Lee, N. Lee, T. Kim, J. Kim and T. Hyeon, *Accounts of Chemical Research*, 2011, **44**, 893-902.
34. K. M. Marks and G. P. Nolan, *Nat Methods*, 2006, **3**, 591-596.
35. M. Helle, E. Rampazzo, M. Monchanin, F. Marchal, F. Guillemin, S. Bonacchi, F. Salis, L. Prodi and L. Bezdetnaya, *ACS-Nano*.
36. X. T. Zheng and C. M. Li, *Chem Soc Rev*, 2012, **41**, 2061-2071.
37. E. Rampazzo, S. Bonacchi, D. Genovese, R. Juris, M. Marcaccio, M. Montalti, F. Paolucci, M. Sgarzi, G. Valenti, N. Zaccheroni and L. Prodi, *Coord. Chem. Rev.*, 2012, **256**, 1664-1681.
38. A. Roda, M. Di Fusco, A. Quintavalla, M. Guardigli, M. Mirasoli, M. Lombardo and C. Trombini, *Anal Chem*, 2012, **84**, 9913-9919.
39. L. Yuan, W. Lin, K. Zheng and S. Zhu, *Accounts of Chemical Research*, 2013, **46**, 1462-1473.
40. S. Mukhopadhyay and A. A. Deniz, *J Fluoresc*, 2007, **17**, 775-783.
41. P. K. Dutta, R. Varghese, J. Nangreave, S. Lin, H. Yan and Y. Liu, *J Am Chem Soc*, 2011, **133**, 11985-11993.
42. W. B. O'Dell, K. J. Beatty, J. K.-H. Tang, R. E. Blankenship, V. S. Urban and H. O'Neill, *Journal of Materials Chemistry*, 2012, **22**, 22582-22591.
43. J. Karolin, L. B. A. Johansson, L. Strandberg and T. Ny, *Journal of the American Chemical Society*, 1994, **116**, 7801-7806.
44. T. Foerster, *Journal of Biomedical Optics*, 2012, **17**.
45. G. Kolbe, *Ph.D. thesis*, 1956.
46. W. Stöber, A. Fink and E. Bohn, *Journal of Colloid and Interface Science*, 1968, **26**, 62-69.
47. A. Van Blaaderen and A. Vrij, *Langmuir*, 1992, **8**, 2921-2931.
48. A. Van Blaaderen, A. Imhof, W. Hage and A. Vrij, *Langmuir*, 1992, **8**, 1514-1517.
49. M. Montalti, L. Prodi, N. Zaccheroni, G. Battistini, S. Marcuz, F. Mancin, E. Rampazzo and U. Tonellato, *Langmuir*, 2006, **22**, 5877-5881.
50. F. J. Arriagada and K. Osseo-Asare, *Journal of Colloid and Interface Science*, 1995, **170**, 8-17.
51. C.-L. Chang and H. S. Fogler, *Langmuir*, 1997, **13**, 3295-3307.
52. H. Ow, D. R. Larson, M. Srivastava, B. A. Baird, W. W. Webb and U. Wiesner, *Nano Letters*, 2004, **5**, 113-117.
53. I. Roy, T. Y. Ohulchanskyy, H. E. Pudavar, E. J. Bergey, A. R. Oseroff, J. Morgan, T. J. Dougherty and P. N. Prasad, *Journal of the American Chemical Society*, 2003, **125**, 7860-7865.
54. D. J. Bharali, I. Klejbor, E. K. Stachowiak, P. Dutta, I. Roy, N. Kaur, E. J. Bergey, P. N. Prasad and M. K. Stachowiak, *Proceedings of the National Academy of Sciences of the United States of America*, 2005, **102**, 11539-11544.
55. K. Ma, U. Werner-Zwanziger, J. Zwanziger and U. Wiesner, *Chemistry of Materials*, 2013, **25**, 677-691.
56. R. P. Bagwe, C. Yang, L. R. Hilliard and W. Tan, *Langmuir*, 2004, **20**, 8336-8342.
57. R. P. Bagwe, L. R. Hilliard and W. Tan, *Langmuir*, 2006, **22**, 4357-4362.
58. S. Kim, T. Y. Ohulchanskyy, H. E. Pudavar, R. K. Pandey and P. N. Prasad, *Journal of the American Chemical Society*, 2007, **129**, 2669-2675.
59. R. Kumar, I. Roy, T. Y. Ohulchanskky, L. A. Vathy, E. J. Bergey, M. Sajjad and P. N. Prasad, *ACS Nano*, 2010, **4**, 699-708.
60. K. T. Yong, I. Roy, M. T. Swihart and P. N. Prasad, *Journal of Materials Chemistry*, 2009, **19**, 4655-4672.
61. G. Valenti, E. Rampazzo, S. Bonacchi, T. Khajvand, R. Juris, M. Montalti, M. Marcaccio, F. Paolucci and L. Prodi, *Chem. Commun.*, 2012, **48**, 4187-4189.
62. P. R. Desai, N. J. Jain, R. K. Sharma and P. Bahadur, *Colloids and Surfaces A: Physicochemical and Engineering Aspects*, 2001, **178**, 57-69.
63. E. Rampazzo, S. Bonacchi, R. Juris, M. Montalti, D. Genovese, N. Zaccheroni, L. Prodi, D. C. Rambaldi, A. Zattoni and P. Reschiglian, *The Journal of Physical Chemistry B*, 2010, **114**, 14605-14613.
64. S. Zanarini, E. Rampazzo, S. Bonacchi, R. Juris, M. Marcaccio, M. Montalti, F. Paolucci and L. Prodi, *Journal of the American Chemical Society*, 2009, **131**, 14208-14209.
65. G. Valenti, E. Rampazzo, S. Bonacchi, T. Khajvand, R. Juris, M. Montalti, M. Marcaccio, F. Paolucci and L. Prodi, *Chemical Communications*, 2012, **48**, 4187-4189.
66. E. Rampazzo, F. Boschi, S. Bonacchi, R. Juris, M. Montalti, N. Zaccheroni, L. Prodi, L. Calderan, B. Rossi, S. Becchi and A. Sbarbati, *Nanoscale*, 2012, **4**, 824-830.
67. M. Helle, E. Rampazzo, M. Monchanin, F. Marchal, F. Guillemin, S. Bonacchi, F. Salis, L. Prodi and L. Bezdetnaya, *ACS Nano*, 2013.
68. E. Rampazzo, S. Bonacchi, R. Juris, M. Montalti, D. Genovese, N. Zaccheroni, L. Prodi, D. C. Rambaldi, A. Zattoni and P. Reschiglian, *J. Phys. Chem. B*, 2010, **114**, 14605-14613.
69. B. L. Cushing, V. L. Kolesnichenko and C. J. O'Connor, *Chemical Reviews*, 2004, **104**, 3893-3946.
70. E. Rampazzo, S. Bonacchi, M. Montalti, L. Prodi and N. Zaccheroni, *Journal of the American Chemical Society*, 2007, **129**, 14251-14256.
71. A. Bumb, S. K. Sarkar, X. S. Wu, M. W. Brechbiel and K. C. Neuman, *Biomedical Optics Express*, 2011, **2**, 2761-2769.
72. J. Baumann and M. D. Fayer, *Journal of Chemical Physics*, 1986, **85**, 4087-4107.
73. D. Genovese, S. Bonacchi, R. Juris, M. Montalti, L. Prodi, E. Rampazzo and N. Zaccheroni, *Angew. Chem.*, 2013, **52**, 5965-5968.
74. R. O. Al-Kaysi, T. Sang Ahn, A. M. Muller and C. J. Bardeen, *Phys Chem Chem Phys*, 2006, **8**, 3453-3459.
75. K. A. Colby, J. J. Burdett, R. F. Frisbee, L. Zhu, R. J. Dillon and C. J. Bardeen, *Journal of Physical Chemistry A*, 2010, **114**, 3471-3482.
76. F. Fennel and S. Lochbrunner, *Physical Chemistry Chemical Physics*, 2011, **13**, 3527-3533.
77. S. Zanarini, E. Rampazzo, L. Della Ciana, M. Marcaccio, E. Marzocchi, M. Montalti, F. Paolucci and L. Prodi, *J. Am. Chem. Soc.*, 2009, **131**, 2260-2267.
78. H. Ow, D. R. Larson, M. Srivastava, B. A. Baird, W. W. Webb and U. Wiesner, *Nano Letters*, 2005, **5**, 113-117.

79. D. R. Larson, H. Ow, H. D. Vishwasrao, A. A. Heikal, U. Wiesner and W. W. Webb, *Chemistry of Materials*, 2008, **20**, 2677-2684.
80. M. Beija, C. A. Afonso and J. M. Martinho, *Chem Soc Rev*, 2009, **38**, 2410-2433.
81. L.-C. Ho, C.-M. Ou, C.-L. Li, S.-Y. Chen, H.-W. Li and H.-T. Chang, *Journal of Materials Chemistry B*, 2013, **1**, 2425-2432.
82. M. Ameloot, M. vandeVen, A. U. Acuña and B. Valeur, *Pure and Applied Chemistry*, 2013, **85**, 589-608.
83. N. C. Maiti, M. M. G. Krishna, P. J. Britto and N. Periasamy, *Journal of Physical Chemistry B*, 1997, **101**, 11051-11060.
84. E. Rampazzo, S. Bonacchi, M. Montalti, L. Prodi and N. Zaccheroni, *J. Am. Chem. Soc.*, 2007, **129**, 14251-14256.
85. A. G. L. Olive, A. Del Guerzo, C. Schaefer, C. Belin, G. Raffy and C. Giansante, *Journal of Physical Chemistry C*, 2010, **114**, 10410-10416.
86. J. M. Lim, P. Kim, M.-C. Yoon, J. Sung, V. Dehm, Z. Chen, F. Wuerthner and D. Kim, *Chemical Science*, 2013, **4**, 388-397.
87. A. S. Klymchenko, E. Roger, N. Anton, H. Anton, I. Shulov, J. Vermot, Y. Mely and T. F. Vandamme, *Rsc Advances*, 2012, **2**, 11876-11886.
88. A. J. Kell, M. L. Barnes, Z. J. Jakubek and B. Simard, *The Journal of Physical Chemistry C*, 2011, **115**, 18412-18421.
89. S.-H. Lee, J. Y. Shin, A. Lee and C. Bustamante, *Proceedings of the National Academy of Sciences of the United States of America*, 2012, **109**, 17436-17441.
90. I. L. Medintz, S. A. Trammell, H. Mattoussi and J. M. Mauro, *J Am Chem Soc*, 2004, **126**, 30-31.
91. S. A. Diaz, G. O. Menendez, M. H. Etchehon, L. Giordano, T. M. Jovin and E. A. Jares-Erijman, *Acs Nano*, 2011, **5**, 2795-2805.
92. E. Jares-Erijman, L. Giordano, C. Spagnuolo, K. Lidke and T. M. Jovin, *Molecular Crystals and Liquid Crystals*, 2005, **430**, 257-265.
93. Z. Erno, I. Yildiz, B. Gorodetsky, F. M. Raymo and N. R. Branda, *Photochemical & Photobiological Sciences*, 2010, **9**, 249-253.
94. C. M. Davis, E. S. Childress and E. J. Harbron, *Journal of Physical Chemistry C*, 2011, **115**, 19065-19073.
95. H.-s. Peng, J. A. Stolwijk, L.-N. Sun, J. Wegener and O. S. Wolfbeis, *Angewandte Chemie-International Edition*, 2010, **49**, 4246-4249.
96. J. Peng, X. He, K. Wang, W. Tan, Y. Wang and Y. Liu, *Analytical and Bioanalytical Chemistry*, 2007, **388**, 645-654.
97. Y. H. Chan, M. E. Gallina, X. Zhang, I. C. Wu, Y. Jin, W. Sun and D. T. Chiu, *Anal Chem*, 2012, **84**, 9431-9438.
98. Y. Kim, H. Y. Jung, Y. H. Choe, C. Lee, S. K. Ko, S. Koun, Y. Choi, B. H. Chung, B. C. Park, T. L. Huh, I. Shin and E. Kim, *Angew Chem Int Ed Engl*, 2012, **51**, 2878-2882.
99. J. Chen, P. Zhang, G. Fang, P. Yi, F. Zeng and S. Wu, *J Phys Chem B*, 2012, **116**, 4354-4362.
100. F. May, M. Peter, A. Hutten, L. Prodi and J. Mattay, *Chemistry*, 2012, **18**, 814-821.
101. D. Genovese, M. Montalti, L. Prodi, E. Rampazzo, N. Zaccheroni, O. Tosic, K. Altenhoner, F. May and J. Mattay, *Chem. Commun.*, 2011, **47**, 10975-10977.
102. J. Folling, S. Polyakova, V. Belov, A. van Blaaderen, M. L. Bossi and S. W. Hell, *Small*, 2008, **4**, 134-142.
103. S. Zanarini, E. Rampazzo, S. Bonacchi, R. Juris, M. Marcaccio, M. Montalti, F. Paolucci and L. Prodi, *J. Am. Chem. Soc.*, 2009, **131**, 14208-+.
104. S. Zanarini, M. Felici, G. Valenti, M. Marcaccio, L. Prodi, S. Bonacchi, P. Contreras-Carballada, R. M. Williams, M. C. Feiters, R. J. M. Nolte, L. De Cola and F. Paolucci, *Chem-Eur J*, 2011, **17**, 4640-4647.

Cooperative behaviour in dye-doped nanostructures is obtained through fast energy transfer among dyes, yielding outstanding functionalities for new-generation luminescent probes